

## End-point Control of a Flexible Structure Mounted Manipulator Based on Wavelet Basis Function Networks

David X.P. Cheng

Defence Research and Development Canada - Suffield  
PO Box 4000, Medicine Hat, Alberta T1A 8K6, Canada  
David.Cheng@drdc-rddc.gc.ca

### Abstract

In this paper, we present a wavelet basis function (WBF) network based control scheme for end-point tracking control of a system consisting of a rigid micro manipulator attached at the end of a flexible macro manipulator. The objective is to suppress vibrations in the macro manipulator and at the same time achieve desired motions of the end-effector of the micro manipulator. A WBF network is utilized to approximate the dynamic behavior of the macro-micro manipulator ( $M^3$ ) system in real time, and the controller is developed without any need for prior knowledge of the dynamics. A weight-tuning algorithm for the WBF network is derived using Lyapunov theory. It is shown that both the path tracking error and the damped vibrations are uniformly ultimately bounded under this new control scheme. A case of end-point tracking via kinematic redundancy is studied and the results are compared to those obtained using an MLP network controller and a PD joint controller.

### 1. Introduction

Long-reach manipulators have been proposed for a range of applications that include Space Station maintenance and operation, and nuclear waste disposal. In such applications, the lightweight structure of long-reach manipulators allows the actuators to move faster and carry heavier loads than conventional rigid manipulators. However, the significant structural flexibility makes it difficult to control the position and force at the end-effector accurately and reliably. The incorporation of a small, rigid micro manipulator at the tip of a large, flexible macro manipulator has been proposed as a solution to achieve the desired accurate and robust performance. In order to utilize the macro-micro manipulator ( $M^3$ ) system effectively, one must address the problem of controlling and compensating for vibrations resulting from the flexibility in the macro-manipulator links.

Considerable research has been done to address differ-

ent aspects of the  $M^3$  system. Nenchev *et al.* [1] utilized the reaction null space concept to decompose the joint space of the flexible base and the micro manipulator into orthogonal subspaces such that no vibrations of the flexible base are induced when the end-effector moves along a reactionless reference path. Yoshikawa *et al.* [2] used the redundancy of the  $M^3$  system to generate joint trajectories that enable the micro manipulator to maximize its ability to compensate for the tracking error resulting from the deformation of the macro manipulator. The dynamics of the system are not considered in this control scheme and therefore it is not suitable for a fast tracking control task. Yoshikawa *et al.* [3] modified their previous work by taking into account the system dynamics. However, the problem of closed-loop stability and vibration damping in the macro-manipulator were not addressed in either of these papers. Cheng and Patel [4, 5] proposed a control scheme to suppress vibrations in the macro manipulator while achieving stable desired motions of the end-effector of the micro manipulator. A multi-layer perceptron (MLP) network is utilized to estimate the nonlinear dynamic behavior for the  $M^3$  system, and the resulting estimates are used to develop controllers for the macro and micro manipulators without any need for prior knowledge of the dynamic model of the  $M^3$  system. Under the MLP based control scheme, both the tracking error of the end-effector of the micro manipulator and the vibration in the macro manipulator are rapidly suppressed and constrained within an arbitrarily small vicinity of the origin, while the magnitudes of the joint torques are kept bounded. However, the number of weights required to be adjusted in the MLP network may rapidly increase as the size of the network increases.

To reduce the computational complexity while preserving the advantages of the MLP network based control scheme described above, we propose in this paper to use wavelet basis function (WBF) networks for learning the dynamics of the  $M^3$  system and use the end-point feedback from visual tracking for formulating the joint torque command. The closed-loop stability of the control scheme is guaranteed while fast, precise end-point tracking is

achieved. The performance of the control scheme is studied on a redundant  $M^3$  system working in a 3-D task space.

## 2. Control Schemes Based on Wavelet Basis Function Networks

### 2.1. Tracking Error Dynamics

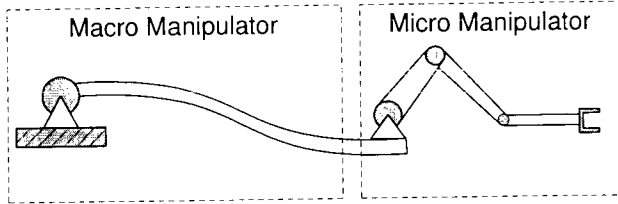


**Figure 1. Schematic of a macro-micro manipulator**

Consider a system consisting of a macro manipulator with  $M$  flexible links and a micro manipulator with  $m$  rigid links (Figure 1) with the equations of motion given by

$$M(x)\ddot{x} + C(x, \dot{x})\dot{x} + G(x) + \tau_d = \tau \quad (1)$$

where  $M$  is the inertia matrix,  $C$  is the matrix of the Coriolis and centrifugal terms,  $G$  is the vector of gravity and elastic torques,  $\tau_d$  represents unmodelled dynamics. The position of the end-effector  $p$  is given by

$$p = p(\theta_M, \theta_m, \delta) \quad (2)$$

where  $\theta_M$  and  $\theta_m$  are the joint positions of the macro and micro arms, respectively, and  $\delta$  is the flexural displacement vector of the macro arm. A small variation in the tip position  $p$  can be expressed as

$$\tilde{p} = J_{\theta_M} \tilde{\theta}_M + J_{\theta_m} \tilde{\theta}_m + J_{\delta} \tilde{\delta} \quad (3)$$

where  $J_{\theta_M} \in \mathbb{R}^{n \times M}$ ,  $J_{\theta_m} \in \mathbb{R}^{n \times m}$  and  $J_{\delta} \in \mathbb{R}^{n \times e}$  are Jacobian matrices of  $p$  with respect to  $\theta_M$ ,  $\theta_m$  and  $\delta$  respectively, and  $\tilde{\theta}_M$ ,  $\tilde{\theta}_m$  and  $\tilde{\delta}$  denote small changes in  $\theta_M$ ,  $\theta_m$  and  $\delta$  respectively.

Denote the desired trajectory as

$$x_d = [\theta_{Md}^T, \theta_{md}^T, \delta_d^T]^T \quad (4)$$

and define the tracking error  $\tilde{x}$  and the filtered tracking error  $r = [r_1^T, r_2^T, r_3^T]^T$  by

$$\tilde{x} \triangleq x - x_d = [\tilde{\theta}_M^T, \tilde{\theta}_m^T, \tilde{\delta}^T]^T \quad (5)$$

$$r_1 \triangleq \dot{\tilde{\theta}}_M + \Lambda_1 \tilde{\theta}_M + \kappa G \dot{\tilde{\delta}} + \Lambda_1 \kappa G \tilde{\delta} \quad (6)$$

$$r_2 \triangleq \dot{\tilde{p}} + \Lambda_2 \tilde{p} \quad (7)$$

$$r_3 \triangleq \dot{\tilde{\delta}} + \Lambda_3 \tilde{\delta} \quad (8)$$

where  $\tilde{\theta}_M = \theta_M - \theta_{Md}$ ,  $\tilde{\delta} = \delta - \delta_d$ ,  $\tilde{\theta}_m = \theta_m - \theta_{md}$ ,  $G$  and  $\Lambda_i, i = 1, 2, 3$ , are symmetric positive-definite matrices,  $\kappa > 0$  is a design parameter. The vector  $r$  can then be expressed in a matrix form

$$r = \Gamma \dot{\tilde{x}} + \tilde{\Gamma} \tilde{x} + \Lambda \Gamma \tilde{x} \quad (9)$$

where  $\Lambda = \text{diag}\{\Lambda_1, \Lambda_2, \Lambda_3\}$  and

$$\Gamma = \begin{bmatrix} I_M & 0 & \kappa G \\ J_{\theta_M} & J_{\theta_m} & J_{\delta} \\ 0 & 0 & I_e \end{bmatrix} \quad (10)$$

with  $\dot{J}_{(\cdot)}$  representing the time derivatives of the Jacobians, and  $I_M$  and  $I_e$  representing the  $M \times M$  and  $e \times e$  identity matrices, respectively. Then the dynamics of the  $M^3$  system can be expressed in terms of the filtered tracking error as

$$M \Upsilon \dot{r} + (C \Upsilon + M \dot{\Upsilon}) r = f - \tau_d + \tau \quad (11)$$

where

$$\Upsilon \triangleq \Gamma^{-1} = \begin{bmatrix} I_M & 0 & -\kappa G \\ -J_{\theta_M}^{-1} J_{\theta_m} & -J_{\theta_m}^{-1} & J_{\theta_m}^{-1} (J_{\delta} - \kappa J_{\theta_M} G) \\ 0 & 0 & I_e \end{bmatrix} \quad (12)$$

and  $f$  is an unknown nonlinear function of parameters such as the inertia, centrifugal and Coriolis terms, DH parameters, etc., of the  $M^3$  system, and is given by

$$f(u) = -G - M \ddot{x}_d - C \dot{x}_d + M \Upsilon (2 \Gamma \dot{\tilde{x}} + \tilde{\Gamma} \tilde{x} + \Lambda (\Gamma \dot{\tilde{x}} + \tilde{\Gamma} \tilde{x})) + C \Upsilon (\tilde{\Gamma} \tilde{x} + \Lambda \Gamma \tilde{x}) + M \dot{\Upsilon} r \quad (13)$$

where  $u$  can be chosen as

$$u \triangleq [\tilde{x}^T, \dot{\tilde{x}}^T, \ddot{x}_d^T, \dot{\tilde{\delta}}^T, \ddot{x}_d^T]^T \quad (14)$$

Expressing the error dynamics as (11) will enable us to derive a WBF network based control scheme in the next section.

### 2.2. Controller Design

Let  $u \in \mathbb{R}^\mu$  and  $f \in \mathcal{L}^2(\mathbb{R}^\mu)$  on a compact set  $\mathcal{S} \subset \mathbb{R}^\mu$ . By the multi-resolution analysis theory [6], for a given positive number  $\epsilon_N > 0$ , there exist a collection of wavelet basis functions  $\{\varphi_{j_0, k} : k \in \mathbb{K}\}$  with a sufficiently small scale  $j_0$  such that

$$f_i(u) = \sum_{k \in \mathbb{K}} c_{i, j_0, k} \varphi_{j_0, k}(u) + \epsilon(u), \quad i = 1, 2, \dots, n \quad (15)$$

and

$$\|\epsilon(u)\| < \epsilon_N, \quad \forall u \in \mathcal{S} \quad (16)$$

where  $\epsilon(u)$  is the reconstruction error and

$$\varphi_{j_0, k}(u) = 2^{-j_0/2} \varphi(2^{-j_0} u - k) \quad (17)$$

$$c_{i, j_0, k} = \langle f_i, \varphi_{j_0, k} \rangle \quad (18)$$

Let  $W = \{c_{i,j_0,k}\}$  and  $\varphi = [\varphi_{j_0,k_1}, \varphi_{j_0,k_2}, \dots, \varphi_{j_0,k_N}]^T$ , where  $k_1, k_2, \dots, k_N$  are the translation vectors in the index set  $\mathbb{K}$ . We can then express (15) in a matrix form:

$$f(u) = W^T \varphi(u) + \varepsilon \quad (19)$$

We assume that on any compact subset of  $\mathbb{R}^n$ , the weighting matrix is bounded, i.e.,

$$\|W\|_F \leq b_W \quad (20)$$

where  $\|\cdot\|_F$  denotes the Frobenius norm. The approximation given by (19) can be implemented by a wavelet basis function (WBF) network. The weights in the input layer of the WBF network are identically set to 1 while the weights in the output layer represent the weighting coefficients of the basis functions  $\varphi_{j_0,k}$  in the wavelet expansion of  $f(u)$  given by (15).

Let an estimate of the nonlinear function  $f(u)$  defined in (13) using a WBF network be given by

$$\hat{f}(u) = \hat{W}^T \varphi(u) \quad (21)$$

where  $\hat{W}$  is an estimate of the weights of the WBF network determined by a tuning algorithm to be specified. Let  $\hat{f}$  be partitioned into  $\hat{f} = [\hat{f}_1^T, \hat{f}_2^T, \hat{f}_3^T]^T$  with  $\hat{f}_1 \in \mathbb{R}^M$ ,  $\hat{f}_2 \in \mathbb{R}^m$  and  $\hat{f}_3 \in \mathbb{R}^e$ . As in the case of the MLP network [4], the structure of the error dynamics given by (11) and the stability analysis motivate us to design the WBF network based controllers for the macro and micro arms of the  $M^3$  system as follows:

$$\tau_M = -\hat{f}_1 + \xi_1 - \frac{\bar{r}_1 \bar{r}_3^T}{\|\bar{r}_1\|^2 + \varepsilon} \cdot (\hat{f}_3 - \xi_3 + K_3 \bar{r}_3) - K_1 \bar{r}_1 \quad (22)$$

$$\tau_m = -\hat{f}_2 + \xi_2 - K_2 \bar{r}_2 \quad (23)$$

$$\xi_i = -k_\xi \frac{\bar{r}_i}{\|\bar{r}_i\|}, \quad i = 1, 2, 3 \quad (24)$$

$$\bar{r} = [\bar{r}_1^T, \bar{r}_2^T, \bar{r}_3^T]^T = \Upsilon r, \quad \bar{r}_1 \in \mathbb{R}^M, \bar{r}_2 \in \mathbb{R}^m, \bar{r}_3 \in \mathbb{R}^e \quad (25)$$

where  $K_i$ ,  $i = 1, 2, 3$ , are positive definite matrices,  $\varepsilon > 0$  and  $k_\xi > 0$  are positive design constants,  $\Upsilon$  is a nonlinear transformation given by (12), and  $\xi_i$ ,  $i = 1, 2, 3$ , are robustifying components incorporated to compensate for the reconstruction errors of the neural network and the unmodelled dynamics.

### 2.3. Weight Tuning Algorithm

Based on the control scheme given by (22) through (25), a weight tuning algorithm for the WBF network can be designed as a natural extension of the weight tuning algorithm for the MLP network developed in [4] for achieving stable

tracking control of the closed-loop flexible  $M^3$  system. The algorithm is determined by the following equation:

$$\dot{\hat{W}} = P(\varphi \cdot \bar{r}^T - \mu \|\bar{r}\| \hat{W}) \quad (26)$$

where  $P = P^T$  is any constant symmetric positive-definite matrix,  $\mu > 0$  is a small scalar design parameter, and  $\Upsilon$  is a nonlinear transformation given by (12). A block diagram of the  $M^3$  control system is shown in Figure 2.

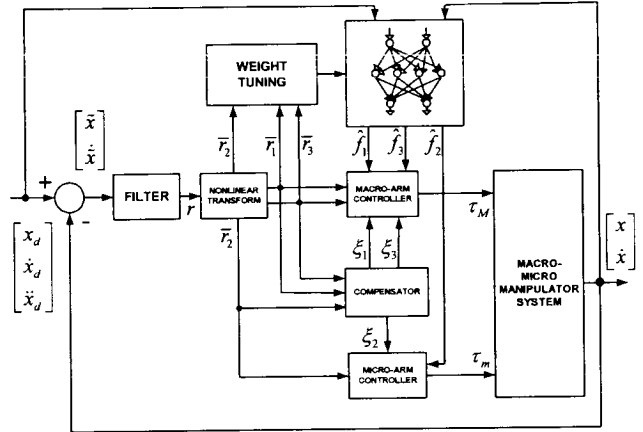


Figure 2. Block diagram of the  $M^3$  control system

### 2.4. Algorithm Analysis

The algorithm presented above is derived by an extension of Lyapunov theory. It can be shown that under the WBF network based control scheme and the weight tuning algorithm proposed above, the tracking errors for the  $M^3$  system can be uniformly driven to an arbitrarily small neighborhood around zero. Choose the Lyapunov function candidate

$$V(r, \bar{W}, t) = \frac{1}{2} r^T \Upsilon^T M \Upsilon r + \frac{1}{2} \text{tr}\{\bar{W}^T P^{-1} \bar{W}\} \quad (27)$$

where  $\text{tr}\{\cdot\}$  denotes the trace of a square matrix. Differentiating  $V$  along the solution of the error dynamics system yields

$$\dot{V} = \frac{1}{2} r^T \Upsilon^T (\dot{M} - 2C) \Upsilon r + r^T \Upsilon^T (f + \tau - \tau_d) + \text{tr}\{\bar{W}^T P^{-1} \dot{\bar{W}}\} \quad (28)$$

Using  $\bar{r} = \Upsilon r$  and the skew-symmetric property of  $\dot{M} - 2C$ , we obtain

$$\dot{V} = \bar{r}_1^T (f_1 + \tau_M) + \bar{r}_2^T (f_2 + \tau_m) + \bar{r}_3^T f_3 - \bar{r}^T \tau_d + \text{tr}\{\bar{W}^T P^{-1} \dot{\bar{W}}\} \quad (29)$$

Substituting the control laws (22) and (23) into the above equation, we obtain

$$\begin{aligned} \dot{V} &= \bar{r}_1^T \left( f_1 - \hat{f}_1 + \xi_1 - \frac{\bar{r}_1 \bar{r}_3^T}{\|\bar{r}_1\|^2 + \varepsilon} (\hat{f}_3 - \xi_3 + K_3 \bar{r}_3) - K_1 \bar{r}_1 \right) \\ &\quad + \bar{r}_3^T f_3 + \bar{r}_2^T (f_2 - \hat{f}_2 + \xi_2 - K_2 \bar{r}_2) - \bar{r}^T \tau_d + \text{tr}\{\bar{W}^T P^{-1} \dot{\bar{W}}\} \\ &\leq -\bar{r}^T K \bar{r} + \bar{r}^T \bar{f} + \bar{r}^T \xi - \bar{r}^T \tau_d + \text{tr}\{\bar{W}^T R^{-1} \dot{\bar{W}}\} \end{aligned} \quad (30)$$

where  $K = \text{diag}\{K_1, K_2, K_3\}$ ,  $\bar{f} = f - \hat{f}$ , and  $\xi = [\xi_1^T, \xi_2^T, \xi_3^T]^T$ . From (19) and (21), the second term on the right-hand side of (30) can be expressed as

$$\begin{aligned} \bar{r}^T \bar{f} &= \bar{r}^T (W^T \varphi - \hat{W}^T \varphi + \varepsilon) \\ &= \bar{r}^T \bar{W}^T \varphi + \bar{r}^T \varepsilon \end{aligned} \quad (31)$$

From (24), the third term on the right-hand side of (30) can be expressed as

$$\begin{aligned} \bar{r}^T \xi &= -\bar{r}^T \cdot k_\xi \frac{\bar{r}}{\|\bar{r}\|} \\ &= -k_\xi \|\bar{r}\| \end{aligned} \quad (32)$$

From (26), the last term on the right-hand side of (30) can be expressed as

$$\begin{aligned} \text{tr}\{\bar{W}^T P^{-1} \dot{\bar{W}}\} &= -\text{tr}\{\bar{W}^T P^{-1} \dot{\bar{W}}\} \\ &= -\text{tr}\{\bar{W}^T P^{-1} P(\varphi \cdot \bar{r}^T - \mu \|\bar{r}\| \hat{W})\} \\ &= -\bar{r}^T \bar{W}^T \varphi + \mu \|\bar{r}\| \text{tr}\{\bar{W}^T \hat{W}\} \end{aligned} \quad (33)$$

Substituting (31), (32) and (33) into (30) we obtain

$$\begin{aligned} \dot{V} &\leq -\bar{r}^T K \bar{r} + \bar{r}^T \bar{W}^T \varphi + \bar{r}^T \varepsilon - k_\xi \|\bar{r}\| - \bar{r}^T \tau_d \\ &\quad - \bar{r}^T \bar{W}^T \varphi + \mu \|\bar{r}\| \text{tr}\{\bar{W}^T \hat{W}\} \\ &\leq -\bar{r}^T K \bar{r} - k_\xi \|\bar{r}\| + \bar{r}^T (\varepsilon - \tau_d) + \mu \|\bar{r}\| \text{tr}\{\bar{W}^T \hat{W}\} \\ &\leq -\bar{r}^T K \bar{r} - k_\xi \|\bar{r}\| + \bar{r}^T (\varepsilon - \tau_d) + \mu \|\bar{r}\| (b_W \|\bar{W}\|_F - \|\bar{W}\|_F^2) \\ &\leq -\|\bar{r}\| \left\{ \lambda_{\min}(K) \|\bar{r}\| + \mu (\|\bar{W}\|_F^2 - b_W \|\bar{W}\|_F) + \varepsilon_N \right\} \end{aligned} \quad (34)$$

where we have applied the known condition  $k_\xi > b_d$  and the inequality  $\text{tr}\{\bar{W}^T \hat{W}\} \leq b_W \|\bar{W}\|_F - \|\bar{W}\|_F^2$  [4] to augment the right-hand side of (34). Completing the squares results in

$$\dot{V} \leq -\|\bar{r}\| \left\{ \lambda_{\min}(K) \|\bar{r}\| + \mu \left( \|\bar{W}\|_F - \frac{b_W}{2} \right)^2 - \frac{\mu b_W^2}{4} + \varepsilon_N \right\} \quad (35)$$

Therefore,  $\dot{V} < 0$  if

$$\|\bar{r}\| > \frac{1}{\lambda_{\min}(K)} \left( \frac{\mu b_W^2}{4} + \varepsilon_N \right) \triangleq b_{\bar{r}} \quad (36)$$

or

$$\|\bar{W}\|_F > \frac{b_W}{2} + \sqrt{\frac{b_W^2}{4} + \frac{\varepsilon_N}{\mu}} \triangleq b_{\bar{W}} \quad (37)$$

Here  $b_r$  and  $b_{\bar{W}}$  denote the regions of convergence for the filtered tracking error and the weight estimation error in the controller, respectively.  $\dot{V}$  becomes negative and  $V$  decreases outside the compact set defined by  $\|r\| \leq b_r$  and  $\|\bar{W}\|_F \leq b_{\bar{W}}$ . According to the LaSalle extension of Lyapunov analysis, this concludes that both  $r$  and  $\bar{W}$  are uniformly ultimately bounded (UUB).

### 3. End-point Tracking by Kinematic Redundancy

To demonstrate the effectiveness of the proposed control scheme, we have applied it to a  $M^3$  system with one flexible boom and four rigid micro-arms. The flexible boom has a thickness of 1.3 mm, width of 3.14 cm, length of 1 m, mass of 1 kg and flexural rigidity of 20 Nm<sup>2</sup>. The first and second rigid links have equal lengths of 0.1 m and equal masses of 0.1 kg, and the third and fourth have equal lengths of 0.2 m and equal masses of 0.2 kg. The assumed-modes method with clamped-mass boundary conditions was used to model the  $M^3$  system. Two orthonormal mode shapes were taken into account for simplifying the inertia and stiffness matrices. The resulting natural frequencies of vibration are 2.50 Hz and 15.6 Hz. The redundancy of the micro manipulator was fully used to suppress vibrations in the flexible boom. All the joints of the  $M^3$  system were controlled to track the end-point trajectory given by

$$\begin{aligned} x_d &= 0.3 \cos(2t) + 0.80 \\ y_d &= \frac{\sqrt{3}}{25\pi} t + 0.5\sqrt{3} \\ z_d &= 0.1 \sin(2t) \end{aligned} \quad (38)$$

which is a helix with a radius of 0.2 m. The desired joint velocity  $\dot{\theta}_d$  is given by

$$\dot{\theta}_d = J^+ \dot{p}_d + (I - J^+ J) \eta, \quad (39)$$

where  $J^+$  is the pseudo-inverse of  $[J_{\theta_M}, J_{\theta_m}]$  and  $\eta$  is an arbitrary  $4 \times 1$  vector. The desired joint trajectory  $\theta_d$  is obtained by integrating the above equation.

A WBF network was designed to approximate the unknown nonlinear function  $f$ . The inputs to the network were taken as  $u = [\bar{x}^T, \bar{x}^T, x_d^T, \dot{x}_d^T, \ddot{x}_d^T]^T$ . Twenty-five hidden units were used in the network with the activation wavelets selected to be the radial Mexican hat functions given by

$$\varphi(\mathbf{u}) = (\mu - \mathbf{u}^T \mathbf{u}) e^{-\mathbf{u}^T \mathbf{u} / 2}, \quad \mathbf{u} \in \mathbb{R}^\mu \quad (40)$$

The WBF network has a total of 150 weights which require no prior knowledge of the parameters either of the  $M^3$  system dynamics, and were simply initialized at zero and updated on-line by the weight tuning algorithm given by (26).

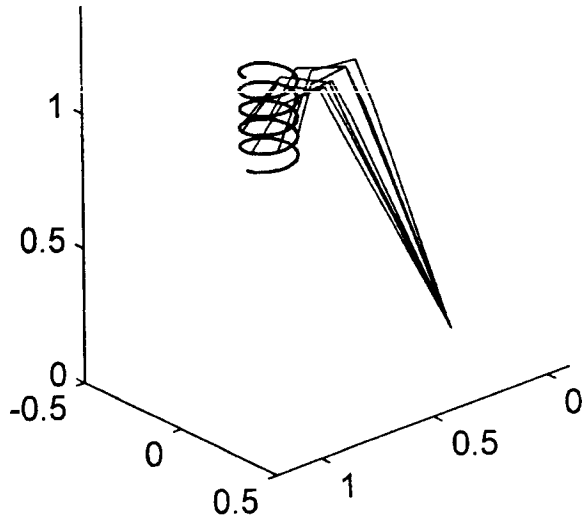


Figure 3. Arm motions of the  $M^3$  system with kinematic redundancy ( $t=3.25-6.25$  sec)

Figure 3 shows the sequences of arm motions controlled by the WBF network for the end-effector of the  $M^3$  system to track the desired helix in 3-D task space. Figures 4 to 6 compare the results of the tracking control of the  $M^3$  system using the WBF network controller against those using an MLP controller [4]. We can see from Figures 4 and 5 that the amount of vibration in the micro arm was effectively constrained in small regions around the origin by the WBF as well as the MLP controller, with the WBF controller being slightly more efficient than the MLP controller in suppressing the vibrations. Figure 6 shows the 2-norms of the task space tracking errors. We can observe that stable and robust tracking were achieved by the MLP and WBF controllers. In this test case, the overall performance of the WBF controller is comparable to that of the MLP controller in the sense of tracking accuracy. Further comparison of the WBF and MLP controllers is provided in Table 1, where we compare the WBF controller with the MLP controller in terms of computational complexity. It can be seen from Table 1 that the total number (150) of weights required to be tuned in the WBF network is much less than that (376) required by the MLP network, which makes the WBF controller faster in learning the dynamics of the  $M^3$  system. Figure 7 compares the tracking errors in task space using the WBF network based controller and a PD controller. The PD controller was implemented by

Table 1. Comparison of the WBF and MLP controllers ( $n_h$ =number of hidden units,  $n_w$ =number of weights,  $n_I$ =number of integrators,  $\|e\|$ =average 2-norm of tracking error)

Item	WBF network	MLP network
$n_h$	25	10
$n_w$	150	376
$n_I$	150	376
$\ e\ $	$8.532 \times 10^{-3}$	$7.296 \times 10^{-3}$

shutting down the WBF network in the outer loop of the system and using the state position and velocity feedback in the inner loop. It is shown that the tracking error is significantly reduced under the proposed WBF network based control scheme. This is because the WBF network controller is capable of suppressing the vibrations in the flexible boom induced by acceleration of the micro manipulator during the end-point tracking.

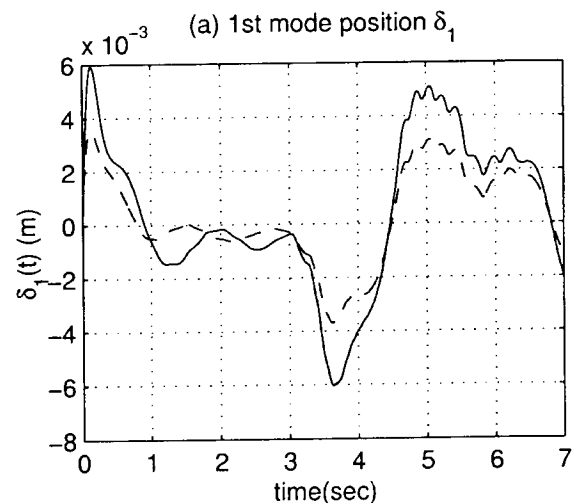


Figure 4. Flexural deflections (1st mode) of the macro manipulator (MLP: —, WBF: - -)

#### 4. Conclusions

In this paper, we present a novel control scheme for time-varying end-point tracking control of a macro-micro manipulator ( $M^3$ ) system based on wavelet basis function

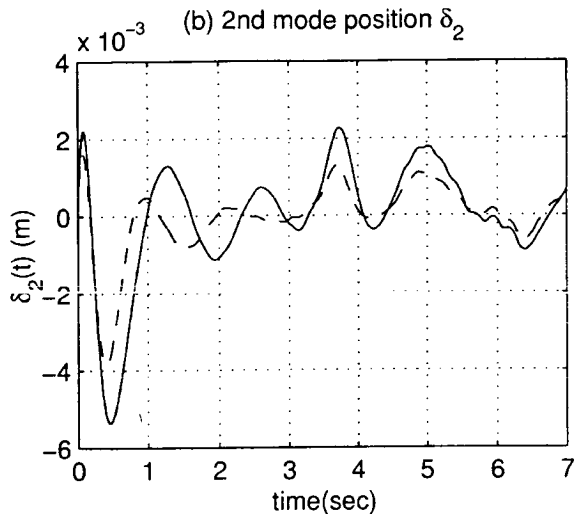


Figure 5. Flexural deflections (2nd mode) of the macro manipulator (MLP network: —, WBF: - -)

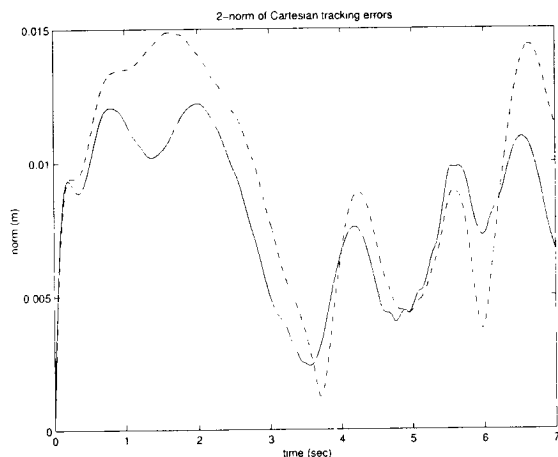


Figure 6. Cartesian tracking errors and error norms (MLP: —, WBF: - -)

(WBF) networks. The control scheme allows us to constrain the tracking errors of the micro manipulator in the presence of vibrations due to the flexibility of the macro manipulator links within an arbitrarily small region around the origin by applying bounded control torques at the joints of the  $M^3$  system. The WBF network is designed to perform the learning and control tasks online simultaneously and no off-line training procedure is required for the neural network to identify the dynamic model of the  $M^3$  system. The stability and convergence properties of the control scheme provide assurances of the reliability needed to make the controller feasible in practical real-time control. The performance of the control scheme is tested and

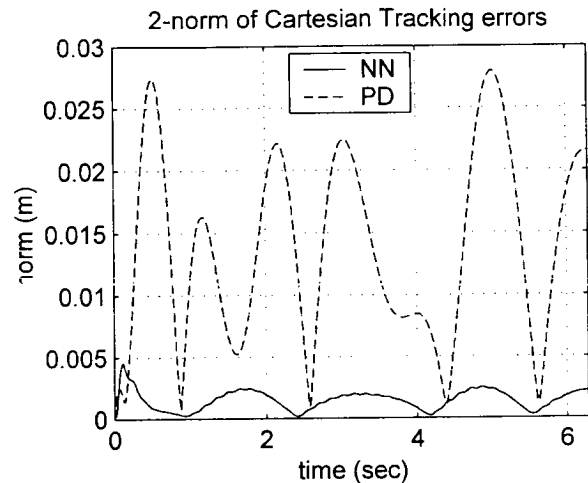


Figure 7. Cartesian tracking errors and error norms (WBF network: —, PD: - -)

compared to that of an MLP network controller and a PD joint controller on a four-link rigid micro manipulator attached at the tip of a flexible structure. It is shown that the WBF network controller significantly improves the tracking performance over the PD controller, and it is capable of achieving comparable performance to that of the MLP controller while significantly reducing the amount of on-line computation for updating the weights of the network.

## References

- [1] D.N. Nenchev, K. Yoshida, P. Vichitkulsawat, and M. Uchiyama, "Reaction null-space control of flexible structure mounted manipulator systems," *IEEE Transactions on Robotics and Automation*, vol. 15, pp. 1011–1023, 1999.
- [2] T. Yoshikawa, K. Hosoda, T. Doi, and H. Murakami, "Quasi-static trajectory tracking control of flexible manipulator by a macro-micro manipulator system," in *Proceedings of the IEEE International Conference on Robotics and Automation*, 1993, pp. 210–215.
- [3] T. Yoshikawa, K. Hosoda, T. Doi, and H. Murakami, "Dynamic trajectory tracking control of flexible manipulator by a macro-micro manipulator system," in *Proc. IEEE Int. Conf. Robotics and Automation*, San Diego, CA, June 1994, pp. 1804–1809.
- [4] D.X.P. Cheng and R.V. Patel, "Neural network based tracking control of a flexible macro-micro manipulator system," *Neural Networks*, vol. 16, pp. 271–286, 2003.
- [5] D.X.P. Cheng and R.V. Patel, "Vibration control of a flexible macro-micro manipulator system using neural networks," in *Proc. 15th IFAC World Congress*, Barcelona, Spain, 2002.
- [6] S.G. Mallat, *A Wavelet Tour of Signal Processing*, Academic Press, New York, NY, 2nd edition, 1999.

# 5240<7

CA 026238